Research Article

Israel Journal of Chemistry
www.ijc.wiley-vch.de

doi.org/10.1002/ijch.202300057

Artificial Siderophores with a Trihydroxamate-DOTAM Scaffold Deliver Iron and Antibiotic Cargo into the Bacterial Pathogen *Escherichia coli*

Isabell Schneider,[a] Verena Fetz,[a] Hans-Peter Prochnow,[a] and Mark Brönstrup*[a, b, c]

Abstract: Infections with multidrug-resistant Gram-negative bacteria constitute a silent pandemic threat that is increasing globally. A major technical and scientific hurdle hampering the development of efficient antibiotics against Gram-negative species is the low permeability of their outer membrane that prevents the entry of most small molecules into the cells. This can be overcome by targeting active iron transport systems of the pathogens in a Trojan-Horse strategy that makes use of drug-loaded artificial siderophores. While we utilized catechols as iron-binding motifs in previous work, this study reports the design, synthesis and characterization of siderophores with a DOTAM scaffold that was substituted with three hydroxamate arms allowing for a hexacoordination of iron. Their iron-chelating capabilities were shown colorimetrically, and the ability of compound **1** to deliver iron into *Escherichia coli* in a chelation-specific manner was proven by a growth recovery assay. A covalent siderophore-ciprofloxacin conjugate exerted antibiotic effects against *E. coli*, albeit it was less potent than the free drug. The study qualifies artificial DOTAM siderophores with hydroxamate binders as scaffolds for bacterial Trojan Horses. This contribution for honoring my mentor Helmut Schwarz echoes two motifs of my work with him: Hydroxylamin, the topic of my first paper ever, and the fascinating properties of iron ions, studied in the gas phase during my Ph.D. Thesis, became a core subject of our current chemical biology research on antiinfectives.

Keywords: Siderophores · antibiotics · iron · drug discovery · targeted delivery

Introduction

Infections with multidrug-resistant bacteria are a growing health care concern, recently coined as a 'silent pandemic'.[1] Antimicrobial resistance does not only impair chances of a successful cure of patients with community-acquired infections, but also puts achievements of modern medicine such as chemotherapy, organ transplantations or other procedures associated with increased infection susceptibility at risk. The problem is exacerbated by a thin, overall insufficient pipeline of novel, resistance-breaking antibiotics.[2] This is particularly true for Gram-negative pathogens, which have an asymmetric outer membrane with a distinct chemical composition that is impermeable for most small 'drug-like' molecules. To gain a more profound scientific understanding of bacterial translocation has been the subject of intense research efforts, as a prerequisite to find treatment solutions.[3] One rational approach deals with targeting one of the entrance gates for nutrients of Gram-negative bacteria in a Trojan-Horse strategy (Figure 1):[4] Ferric iron is essential for bacterial growth, but notoriously scarce in vivo due to the low solubility of the metal and competing iron storage systems of the host.[5] Therefore, bacteria biosynthesize siderophores, low molecular weight ligands with a high affinity for iron that are secreted into the environment, and actively re-imported into bacteria as holo-complexes.[6] By conjugating an antibiotic to the siderophore, a toxic cargo can be smuggled into the pathogen. The success and clinical relevance of this strategy has been recently proven with the launch of cefiderocol (mind the tradename: 'FeTroja'), a catechol-conjugated cephalosporin.[7]

We have embarked on designing artificial siderophores as Trojan Horses, which are featured by advantages such as tunable iron binding motifs, which translates in altered bacterial selectivity, a scalable and efficient synthetic access, and high stability.[8] In particular, the 1,4,7,10-tetraazacyclododecane core, further functionalized to a DOTAM binder (Figure 1), has turned out to be a versatile scaffold for the

[a] *I. Schneider, V. Fetz, H.-P. Prochnow, M. Brönstrup*
Department of Chemical Biology, Helmholtz Centre for Infection Research, Inhoffenstraße 7, 38124 Braunschweig Germany
E-mail: Mark.Broenstrup@helmholtz-hzi.de
[b] *M. Brönstrup*
Institute for Organic Chemistry (IOC), Leibniz Universität Hannover, Schneiderberg 1B, 30167 Hannover, Germany
[c] *M. Brönstrup*
German Center for Infection Research (DZIF), Site Hannover-Braunschweig, Inhoffenstraße 7, 38124 Braunschweig, Germany

Supporting information for this article is available on the WWW under https://doi.org/10.1002/ijch.202300057

Israel Journal of Chemistry

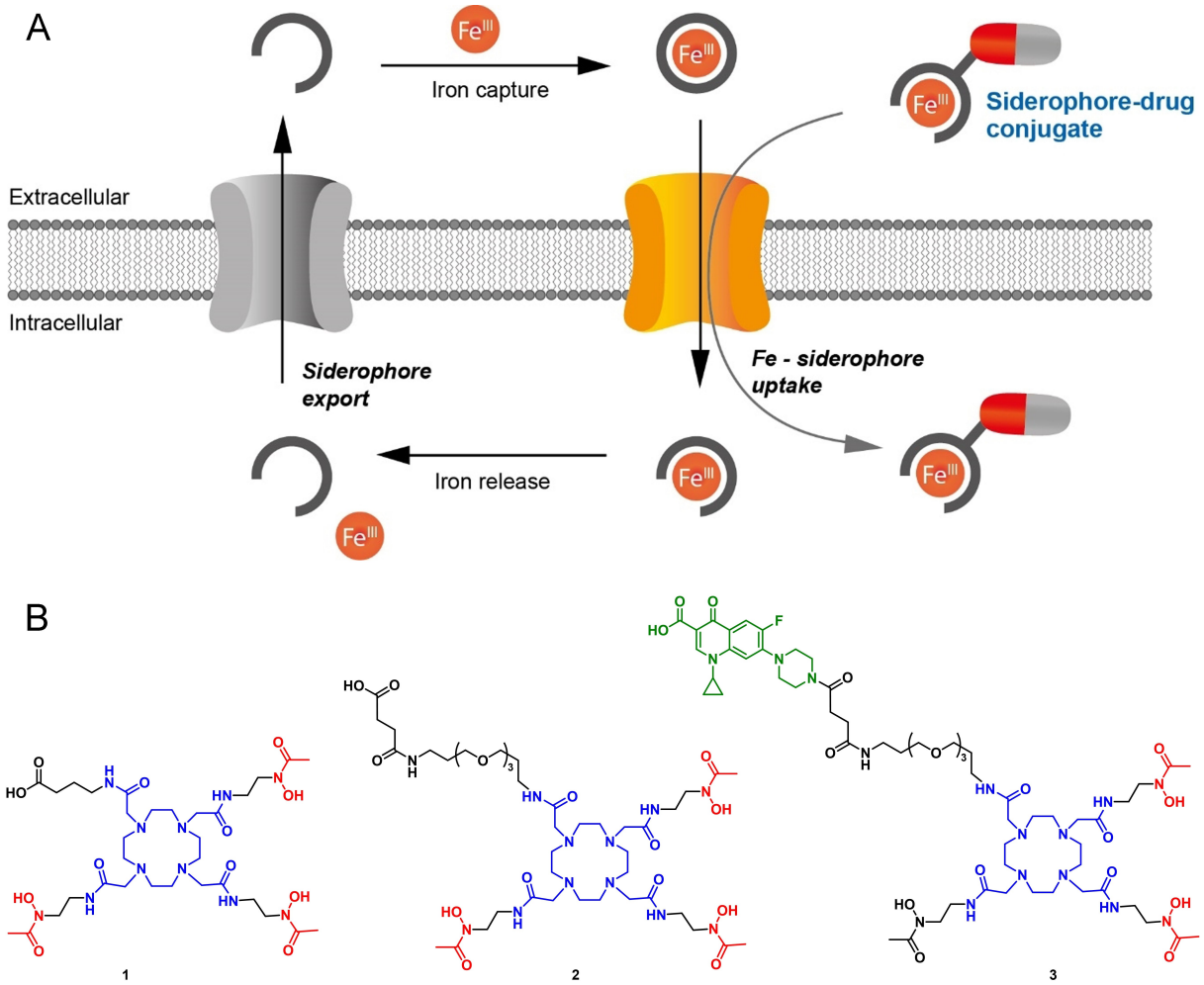

Figure 1. Iron uptake into Gram-negative bacteria and Trojan horse strategy. A) Mechanism of siderophore-mediated iron uptake and its use in Trojan horse conjugates. The siderophore is depicted as a black closed or open circle, and the drug as a grey-red ellipse. B) Structures of **1**, **2**, and **3**. Iron-binding hydroxamates are shown in red, the DOTAM core in blue, and the antibiotic moiety in green.

accommodation of various antibiotics or imaging moieties, that have also been combined to full theranostics.[9] DOTAM-based siderophores proved their functionality in vivo by the imaging of infections in mice by optical as well as positron emission tomography (PET) readouts.[9a,10] So far, we have employed only catechol motifs as iron binders due to their high affinity for the metal; however, they proved to be inferior to linear hydroxamates for the detection of bacteria-triggered chemiluminescent signals due to quenching effects of the catechols.[8a] Furthermore, mechanisms of the innate immune system to inactivate natural catecholate siderophores have been reported,[5,11] and their potentially unspecific binding capabilities towards off-targets constitute further, albeit theoretical concerns. Hydroxamates, on the other hand, have been applied successfully in a variety of siderophore conjugates.[4a,12] For these reasons, the present study aimed at introducing hydroxamates instead of catechols at the established DOTAM core. The synthesis and the biological characterization of a [3 + 1]-substituted DOTAM, substituted with three hydroxamate arms for iron binding and a fourth for the attachment of an antibiotic, is described in the following.

Results and Discussion

In order to assure a tight iron binding, a trihydroxamate ligand that can achieve a hexacoordination of iron was selected. The use of the cyclen scaffold, further functionalized to a DOTAM moiety, allowed the attachment of four substituents. Three of them were used to accommodate three identical, *N*-acetylated hydroxamates, while the fourth substituent served to attach an antibiotic cargo via a linker of appropriate length. We chose to target one siderophore with a relatively short γ-aminobutyric acid linker, i.e. compound **1**, and a second one with a longer triple-PEG-succinate linker, i.e. compound **2** (Figure 1). To obtain a first DOTAM-based trihydroxamate-antibiotic conjugate, a simple covalent connection to the gyrase inhibitor ciprofloxacin to give conjugate **3** was attempted. Although

Israel Journal of Chemistry

ciprofloxacin is a potent antibiotic with Gram-negative activity that does not require uptake enhancement in sensitive strains, it is a good test case to probe whether the conjugates are able to deliver cargo to the cytoplasm, which turned out to be challenging in the past.

The longer triple-PEG-succinate linker was chosen to solubilize the compound and to provide a spacer of 14 Å, because the two quinolone-binding sites in the target, the bacterial gyrase, are centered within a tetrameric protein complex of the enzyme,[13] and might interfere with a directly attached, bulky siderophore. Moreover, there was precedence for the successful use in other ciprofloxacin conjugates.[14]

Retrosynthetically, the target compound **3** should be obtained via amide coupling of ciprofloxacin to **4** (Scheme 1). The linker-extended, protected siderophores **4** and **5** can be traced back to the central intermediate **6**, which is accessible by a threefold alkylation of 1,4,7,10-tetraazacyclododecane (also called cyclen) with the benzyl-protected monohydroxamate **7**. The latter should be obtained from *N*-Boc-ethanolamine **8**.

In the forward direction, **8** was oxidized by freshly prepared IBX to the corresponding aldehyde (Scheme 2). The crude oil was immediately used in the subsequent oxime formation and reductive amination without an intermediate work-up to avoid by-product formation.[15] For the introduction of the acetyl group, the amine was highly concentrated in pyridine and acetic anhydride to reduce the volume of these reagents. Acetic acid was removed through a basic aqueous work-up, and pyridine was extracted washing the organic phase with $CuSO_4$ solution. Starting from **8**, the first intermediate **9** was obtained with a yield of 64%. The presence of 20% TFA in DCM was sufficient to remove the Boc protection group. Finally, the simultaneous addition of an aqueous solution of K_2CO_3 and a solution of bromoacetyl bromide in DCM to the TFA-salt **10** gave the desired product **7** in 38% yield after purification. We observed **11** as a major by-product that probably resulted from a nucleophilic attack of **10** to a mixed anhydride, formed by the attack of TFA to bromoacetyl bromide.

Three molecules of **7** were attached to 1,4,7,10- tetraazacyclododecane **12** in the presence of the base NaOAc in DMA via a SN_2 reaction, (Scheme 3). Using a 3.3 : 1 ratio of **7** to **12** resulted in highest yields (39%) of the trihydroxamate **6**. In the next steps, either the benzyl-protected GABA linker **13** or the triple-ethylene glycol succinate linker **14** were introduced under basic conditions to yield **15** and **16**, respectively. In the substitution reaction with the longer linker, a succinimid was formed as a by-product, while the formation of a glutarimid

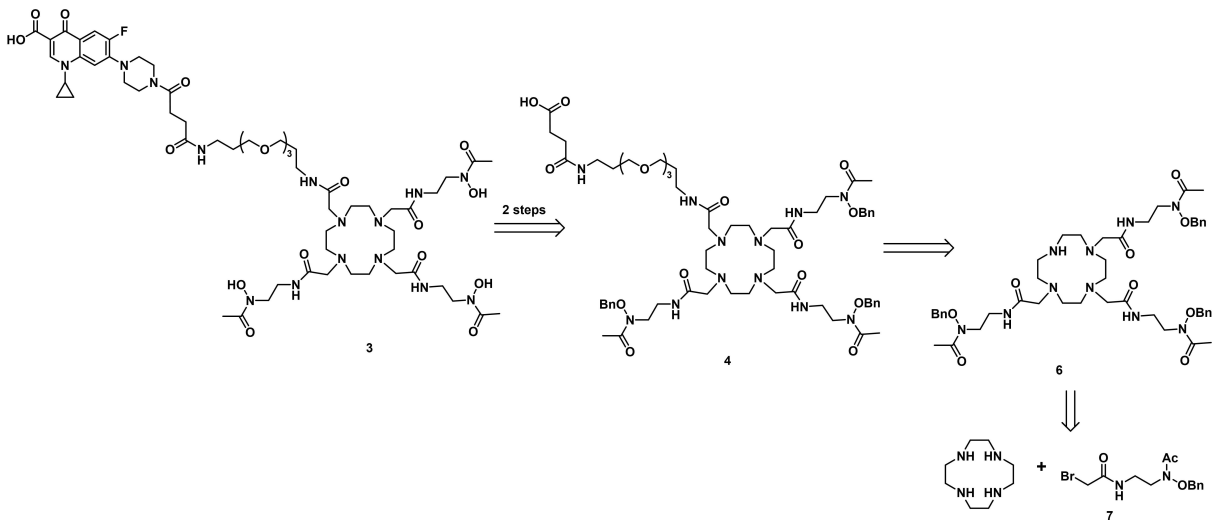

Scheme 1. Retrosynthetic approach for the synthesis of the trihydroxamate siderophores **1** and **2** and the ciprofloxacin conjugate **3**.

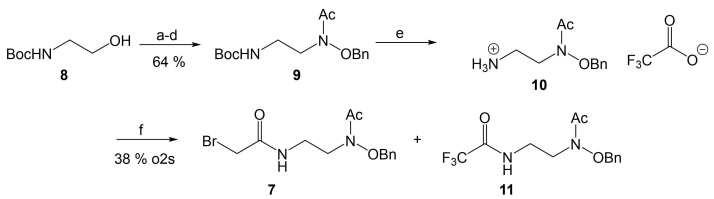

Scheme 2. Synthesis of the brominated and protected hydroxamate **7**. Reagents and conditions: (a) IBX, EtOAc, rflx., 2 h 15 min (b) *O*-benzylhydroxylamine, pyridine, 0–31 °C, 2.5 h (c) $NaCNBH_3$, AcOH, 10–26 °C, 3 h (d) Ac_2O (10 eq.), pyridine (11 eq.), 26 °C, 14.5 h (e) 20% TFA in DCM, 0–27 °C, 1 h (f) $BrCOCH_2Br$, K_2CO_3, 0–22 °C, 1.5 h. o2s = over two steps.

Israel Journal of Chemistry

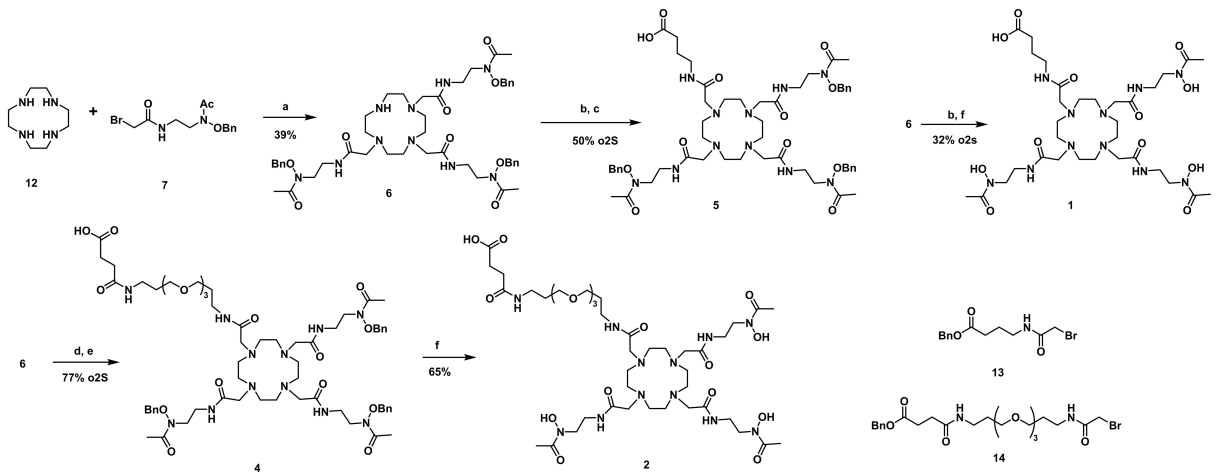

Scheme 3. Synthesis of DOTAM-trihydroxymates **1** and **2**. (a) NaOAc, **7** (3.3 eq), DMA, 24 °C, 19 h; (b) K_2CO_3, **13**, MeCN, 0–26 °C, 2 h (c) NaOH (1 M)/THF (1 : 3), 0–29 °C, 1.5 h; (d) as in (b), with **14**, 0–15 °C, 1 h; (e) NaOH (1 M)/THF (1 : 3), 0 °C, 1 h; (f) 10% Pd/C, H_2, MeOH, 26 °C. o2s = over two steps

was not observed for the shorter linker. The carboxylic acids **5** and **4** were obtained by saponification of the benzyl esters with aqueous NaOH. Overall, **5** and **4** were synthesized in a four-step procedure from **12** in yields of 51% and 77%, respectively. The intermediates were not purified, as the tetrahydroxamate by-product from the first step was difficult to separate at an earlier stage. The siderophores **1** and **2** carrying free hydroxamates were then afforded by Pd-catalyzed hydrogenations.

The benzyl-protected ciprofloxacin precursor **17** was coupled to **4** following a modified procedure from Wencewicz et al. (Scheme 4).[16] Instead of removing TFA from **17** by ion exchange prior to the coupling, ciprofloxacin was deprotonated with DIPEA. The carboxylic acid **4** was activated with DIPEA, DMAP and EDC hydrochloride, and then reacted with deprotonated **17**, affording the coupling product **18** in 59% yield. Finally, the benzyl groups from **18** were removed by a Pd-catalyzed hydrogenation to obtain the ciprofloxacin-conjugate **3** in quantitative yield.

We next characterized the physical and biological properties of the free siderophores and the antibiotic conjugate. Due to a charge transfer from the ligand to the metal, ferric siderophore complexes are of intense color.[17] This characteristic was used to determine whether the DOTAM-based trihydroxamates **1** and **2** chelated Fe(III) in solution. As negative controls, the benzyl-protected hydroxamates **5** and **4** were used. The absorbance of the four compounds was measured in aqueous solution (pH 6) at different concentrations of $FeCl_3$. A maximum absorption at a wavelength of 470 nm was found for the ferric complexes of **1** and **2**, which were both of deep orange color, whereas for **5** and **4**, no complex formation was observed (Figure 2). The experiment demonstrates that **1** and **2** coordinated Fe(III). In addition to the hydroxamates, the DOTAM core represents a second metal binding site. However, previous studies have demonstrated that iron coordination proceeds much slower at the core,[9a] and the fact that the analogous benzyl-protected compounds **5** and **4** did not form such complexes strongly implies that the metal

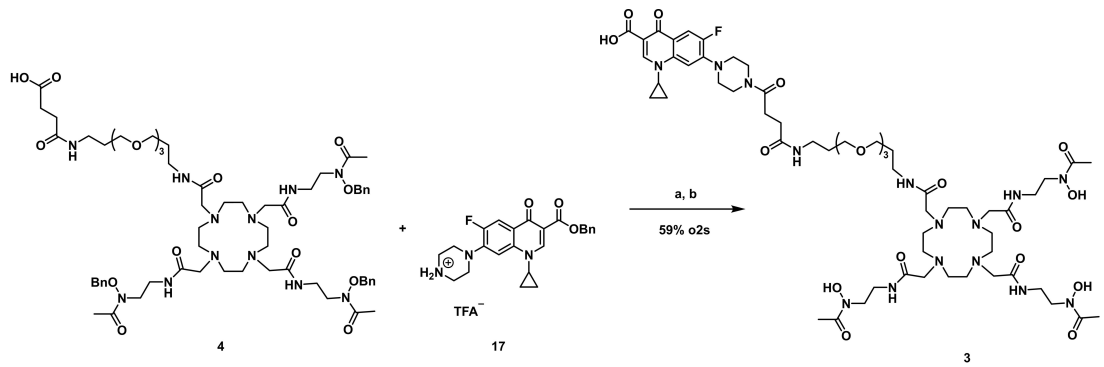

Scheme 4. Synthesis of **3**. (a) DIPEA, DMAP, EDC-HCl, DCM, 0–26 °C, 30 min; then **17** (that was pretreated with DIPEA), DMF, 26 °C, 3 h; (b) 10% Pd–C, H_2, MeOH, 25 °C, 17 h. o2s = over two steps

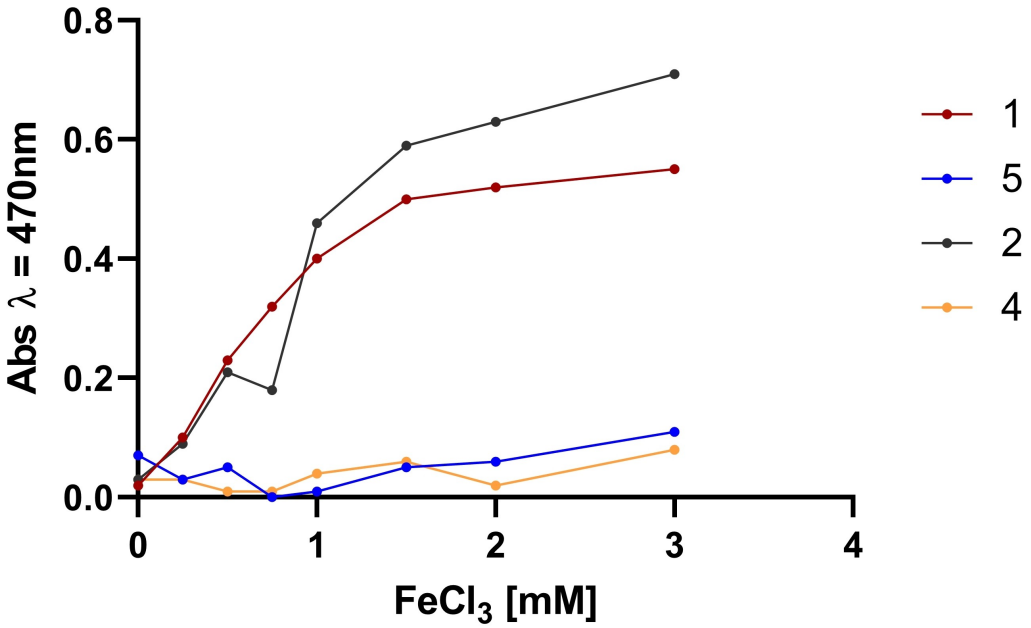

Figure 2. Compounds **1** and **2** coordinate Fe(III) by their hydroxamate moieties. Aqueous, 1 mM solutions of **1** and **2** and of their respective benzyl-protected analogues **5** and **4** were prepared with different concentrations of $FeCl_3$ (0–3 mM) at a final pH of 5–6. After 1 h and 48 h of incubation at 25 °C in the dark, the absorption of the complexes at 470 nm was measured.

was coordinated through free hydroxamate functionalities. In a previous study on releated, DOTAM-based tricatecholates, we have measured a 1 : 1 stochiometry for Fe:ligand by mass spectrometry.[9a] Because this composition was also observed for other, linear iron-binding tri-hydroxamates,[4b] we assume that also **1**, **2**, and further functionalized DOTAM-trihydroxamates reported herein bind iron in a 1 : 1 stochiometry.

Next, we probed whether the putative siderophore **1** was indeed functional, i. e. able to transport iron into bacteria. For this purpose, growth recovery assays with an *E. coli* wildtype (wt) and an *E. coli ΔentA* mutant strain were performed. The gene *entA* encodes 2,3-dihydro-2,3-dihydroxybenzoate dehydrogenase, an essential enzyme for the biosynthesis of enterobactin.[18] Being devoid of its only, endogeneous siderophore enterobactin, *E. coli ΔentA* does not grow at low iron concentrations in the medium ($c(Fe(III) < 10^{-4}$ M), unless a potent exogenous siderophore is provided that assumes the delivery of iron into the cell. We investigated whether the artificial siderophore **1** could recover growth for this strain (Figure 3). As positive controls, the trihydroxamate ferrichrome and the tricatecholate enterobactin and an analogous artificial DOTAM tricatecholate[9a] were tested, whereas DMSO served as a negative control. While *E. coli ΔentA* did not grow when treated with DMSO alone, all three positive control compounds restored growth of the mutant strain, as expected (Figure 3). Remarkably, also **1** recovered growth in the mutant strain, although slightly less than the analogous DOTAM tricatecholate or the other positive controls. The wild type strain grew under all conditions, demonstrating that there were no confounding antibiotic effects under the experimental conditions. The experiments demonstrate that **1** was accepted as a siderophore and delivered iron into *E. coli.*

To test whether the trihydroxamate ciprofloxacin-conjugate **3** possessed antimicrobial activity, the growth of *E. coli* was measured at increasing concentrations of **3**, and the respective half-maximal inhibitory concentration (IC_{50}) was determined. The free siderophore **2** was tested as a control, in order to exclude that the carrier itself contributed to an antibiotic activity. The parent antibiotic ciprofloxacin, known to be highly active against *E. coli*, served as a positive control. An IC_{50} of 34.5 μM was obtained for the sideromycin **3** (Figure 4). For the free siderophore **2**, an IC_{50} could not be determined, thereby verifying that it did not inhibit growth. This demonstrates that the growth inhibition of **3** is caused by the payload ciprofloxacin. Because its target is located in the cytoplasm, it also implies that **3** was able to reach the cytoplasm. However, the potency of **3** was much lower than that of free ciprofloxacin ($IC_{50} = 0.002$ μM).

In order to probe whether iron limitation changed the activity of the synthesized sideromycin the experiment was repeated, but the growth medium was supplemented with 2,2'-bipyridyl (BP) to chelate Fe(III). For the sideromycin **3** and ciprofloxacin, the IC_{50} values remained almost constant. We hypothesize that the wild type strain strongly upregulated the biosynthesis of enterobactin under iron-deficient conditions,[4c,6,19] thereby circumventing an increased uptake of and sensitivity towards **3**. To analyze how enterobactin biosynthesis and transport affected the antimicrobial activity of **3**, the IC_{50} values for the *E. coli* mutant strains *ΔentA* and *ΔentB* were measured in the same setting (Figure 5). *E. coli*

Israel Journal of Chemistry

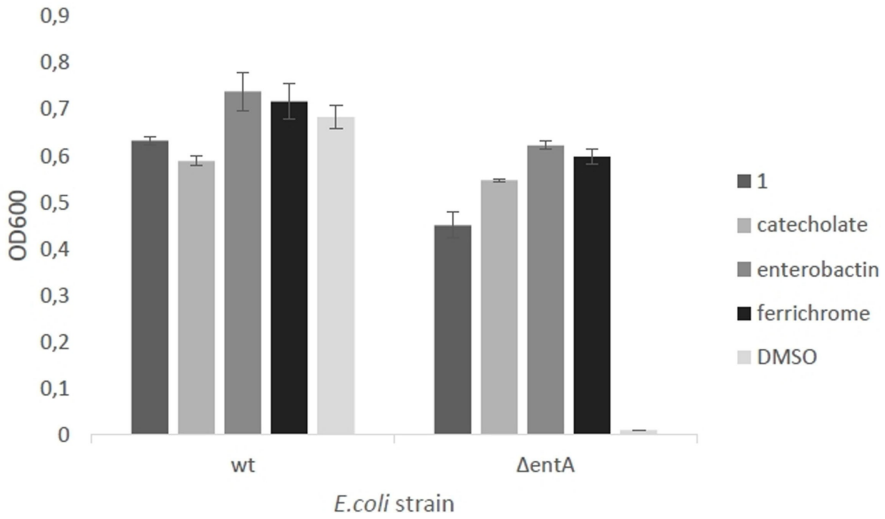

Figure 3. Growth recovery assay with *E. coli* wild type (wt) and *E. coli ΔentA*. The siderophore concentration was 10 μM, and iron chloride concentration was 100 μM. An equivalent volume of pure DMSO was added to cultures for the negative control. OD_{600} was determined after 48 h of incubation. For every condition, four technical replicates were prepared, error bars indicate standard deviations.

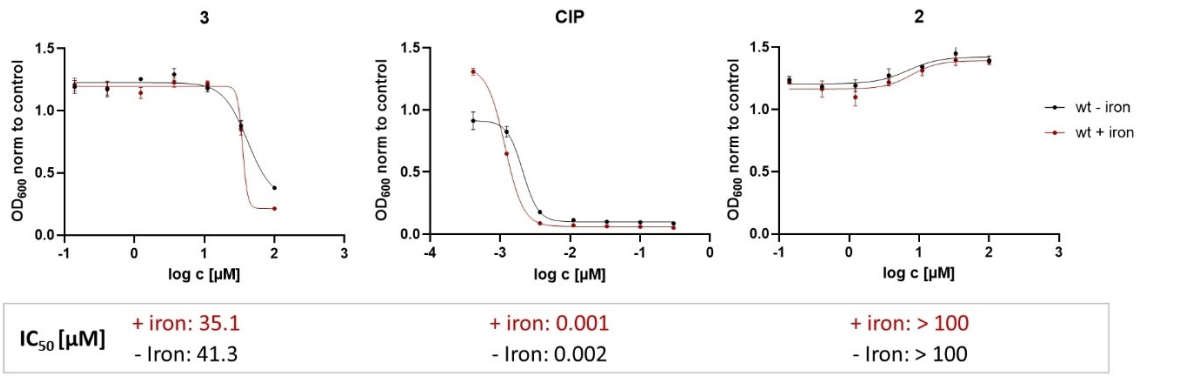

Figure 4. Antimicrobial activity of **3** against *E. coli* wild type. The half maximal inhibitory concentration (IC_{50}) of the **3** was determined using iron-rich Müller-Hinton medium without (+ iron) and with addition of 200 μM 2,2'-bipyridyl to chelate iron from the medium (− iron). Compound **2** was used as a negative control, and the parent antibiotic ciprofloxacin as positive control. Three technical replicates were prepared. IC_{50}-values in μM were determined with GraphPadPrism using 4-parameter logistics and are depicted below the dose-response plots.

mutants *ΔentA* and *ΔentB* lack two essential genes for the enterobactin biosynthesis. In the *ΔentA* and *ΔentB* strains, uptake of **3** should be promoted, as the bacteria rely on exogenous siderophores upon limited iron in the medium. Consequently, we expected **3** to be more active in the strains due to a lack of competition by enterobactin. This hypotheses was confirmed, because the IC_{50} values for **3** were 7.5 μM and 10.1 μM under normal conditions and 2.3 μM and 3.9 μM under iron-limiting conditions in the *ΔentA* and *ΔentB* strains, respectively.

Conclusions

The experiments demonstrate that the artificial hydroxamate siderophore **2** is suited to transport iron and other cargo into *E. coli*. The antibiotic activity of **3** suggests that even the bacterial cytosol is reached, because the target of ciprofloxacin, the bacterial gyrase, is located there. While the compounds validate the concept, they do not represent a practical solution in terms of an antibiotic lead compound. In fact, the conjugates were far less potent than free ciprofloxacin, a gold standard that has no translocation issue. Recent data we obtained with DOTAM-catecholates imply that while transport across the outer membrane was efficient, crossing the inner membrane was not.[9b] This finding is in line with reports

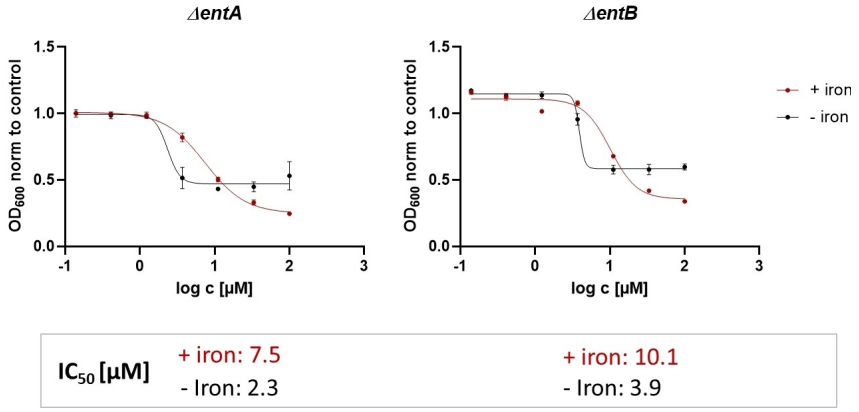

Figure 5. Growth inhibitory activity of **3** in *E. coli* mutant strains. Strains were deficient in enterobactin biosynthesis (*ΔentA* and *ΔentB*). The half maximal inhibitory concentration (IC_{50}) of **3** was determined using iron-rich Müller-Hinton medium without (+ iron) and with addition of 200 μM 2,2'-bipyridyl to chelate iron from the medium (− iron). Three technical replicates were prepared. IC_{50}-values in μM were determined with GraphPadPrism using 4-parameter logistics and are depicted below the dose-response plots.

on other siderophores with covalently bound ciprofloxacins that all displayed antibiotic efficacies that could not reach the level of the free drug overall.[4b] A promising and viable solution is to replace the stable covalent linker with a cleavable, self-immolative moiety, that releases the antibiotic once translocated across the outer membrane. Cleavable linkers incorporating β-lactams,[20] the trimethyl lock,[12e,21] disulfides,[22] hydroxamates[23] or protease cleavage sites[12a,24] have been implemented in other conjugates that showed potent antibacterial activities. Alternatively, the pre-complexation of gallium ions instead of iron has augmented antibiotic effects.[12a–c] While the incorporation of a cleavage site and the extension to other or additional antibiotic moieties are attractive next steps for chemistry, an extended microbiological characterization across further pathogens, such as those from the ESKAPE panel, as well as the mass spectrometric quantification of uptake into the major cell compartments[25] are indicated to further validate DOTAM-based hydroxamate siderophores as Trojan horses in the fight against bacterial infections.

On a personal note, this contribution for honoring Helmut Schwarz echoes two motifs of my work with him: The N–O bond was the topic of my very first paper,[26] and the properties of iron ions, studied in the gas phase during my Ph.D. Thesis, were fascinating ever since.[27] I am grateful for his profound education and inspiration that sustained over time, fueling research that evolved from the gas phase in an unpredictable manner to studying iron in the chemical biology of anti-infectives today.

Acknowledgements

We would like to acknowledge Dr. Kevin Ferreira and Dr. Philipp Klahn for providing valuable advice on synthetic problems, and Ulrike Beutling for measuring high resolution mass spectra. Open Access funding enabled and organized by Projekt DEAL.

Data Availability Statement

The data that support the findings of this study are available in the supplementary material of this article.

References

[1] C. J. L. Murray, K. S. Ikuta, F. Sharara, et al., *Lancet* **2022**, *399*, 629–655.

[2] a) M. S. Butler, V. Gigante, H. Sati, S. Paulin, L. Al-Sulaiman, J. H. Rex, P. Fernandes, C. A. Arias, M. Paul, G. E. Thwaites, L. Czaplewski, R. A. Alm, C. Lienhardt, M. Spigelman, L. L. Silver, N. Ohmagari, R. Kozlov, S. Harbarth, P. Beyer, *Antimicrob. Agents Chemother.* **2022**, *66*, e01991-21; b) U. Theuretzbacher, S. Gottwalt, P. Beyer, M. Butler, L. Czaplewski, C. Lienhardt, L. Moja, M. Paul, S. Paulin, J. H. Rex, L. L. Silver, M. Spigelman, G. E. Thwaites, J. P. Paccaud, S. Harbarth, *Lancet Infect. Dis.* **2019**, *19*, e40-e50; c) M. Miethke, M. Pieroni, T. Weber, M. Brönstrup, P. Hammann, L. Halby, P. B. Arimondo, P. Glaser, B. Aigle, H. B. Bode, R. Moreira, Y. Li, A. Luzhetskyy, M. H. Medema, J. L. Pernodet, M. Stadler, J. R. Tormo, O. Genilloud, A. W. Truman, K. J. Weissman, E. Takano, S. Sabatini, E. Stegmann, H. Brötz-Oesterhelt, W. Wohlleben, M. Seemann, M. Empting, A. K. H. Hirsch, B. Loretz, C. M. Lehr, A. Titz, J. Herrmann, T. Jaeger, S. Alt, T. Hesterkamp, M. Winterhalter, A. Schiefer, K. Pfarr, A. Hoerauf, H. Graz, M. Graz, M. Lindvall, S. Ramurthy, A. Karlén, M. van Dongen, H. Petkovic, A. Keller, F. Peyrane, S. Donadio, L. Fraisse, L. J. V. Piddock, I. H. Gilbert, H. E. Moser, R. Müller, *Nat. Chem. Rev.* **2021**, 1–24.

[3] a) J. D. Prajapati, U. Kleinekathöfer, M. Winterhalter, *Chem. Rev.* **2021**, *121*, 5158–5192; b) H. I. Zgurskaya, V. V. Rybenkov, *Ann. N. Y. Acad. Sci.* **2020**, *1459*, 5–18.

[4] a) M. J. Miller, R. Liu, *Acc. Chem. Res.* **2021**, *54*, 1646–1661; b) P. Klahn, M. Bronstrup, *Nat. Prod. Rep.* **2017**, *34*, 832–885; c) U. Bilitewski, J. A. V. Blodgett, A.-K. Duhme-Klair, S. Dallavalle, S. Laschat, A. Routledge, R. Schobert, *Angew. Chem. Int. Ed.* **2017**, *56*, 14360–14382.
[5] C. C. Murdoch, E. P. Skaar, *Nat. Rev. Microbiol.* **2022**, *20*, 657–670.
[6] M. Miethke, M. A. Marahiel, *Microbiol. Mol. Biol. Rev.* **2007**, *71*, 413-++.
[7] a) R. G. Wunderink, Y. Matsunaga, M. Ariyasu, P. Clevenbergh, R. Echols, K. S. Kaye, M. Kollef, A. Menon, J. M. Pogue, A. F. Shorr, J. F. Timsit, M. Zeitlinger, T. D. Nagata, *Lancet Infect. Dis.* **2021**, *21*, 213–225; b) G. G. Zhanel, A. R. Golden, S. Zelenitsky, K. Wiebe, C. K. Lawrence, H. J. Adam, T. Idowu, R. Domalaon, F. Schweizer, M. A. Zhanel, P. R. S. Lagacé-Wiens, A. J. Walkty, A. Noreddin, J. P. Lynch Iii, J. A. Karlowsky, *Drugs* **2019**, *79*, 271–289.
[8] a) C. Peukert, S. Popat Gholap, O. Green, L. Pinkert, J. van den Heuvel, M. van Ham, D. Shabat, M. Brönstrup, *Angew. Chem. Int. Ed.* **2022**, *n.a.*, e202201423; b) L. Pinkert, Y. H. Lai, C. Peukert, S. K. Hotop, B. Karge, L. M. Schulze, J. Grunenberg, M. Brönstrup, *J. Med. Chem.* **2021**, *64*, 15440–15460.
[9] a) K. Ferreira, H. Y. Hu, V. Fetz, H. Prochnow, B. Rais, P. P. Muller, M. Bronstrup, *Angew. Chem. Int. Ed.* **2017**, *56*, 8272–8276; b) C. Peukert, K. Rox, B. Karge, S. K. Hotop, M. Brönstrup, *ACS Infect. Dis.* **2023**, *9*, 330–341; c) C. Peukert, V. Gasser, T. Orth, S. Fritsch, V. Normant, O. Cunrath, I. J. Schalk, M. Brönstrup, *J. Med. Chem.* **2023**, *66*, 553–576; d) S. Fritsch, V. Gasser, C. Peukert, L. Pinkert, L. Kuhn, Q. Perraud, V. Normant, M. Brönstrup, I. Schalk, *ACS Infect. Dis.* **2022**, *8*, 1134–1146.
[10] C. Peukert, L. N. B. Langer, S. M. Wegener, A. Tutov, J. P. Bankstahl, B. Karge, F. M. Bengel, T. L. Ross, M. Brönstrup, *J. Med. Chem.* **2021**, *64*, 12359–12378.
[11] T. H. Flo, K. D. Smith, S. Sato, D. J. Rodriguez, M. A. Holmes, R. K. Strong, S. Akira, A. Aderem, *Nature* **2004**, *432*, 917–921.
[12] a) A. Pandey, D. Śmiłowicz, E. Boros, *Chem. Sci.* **2021**, *12*, 14546–14556; b) A. Pandey, C. Savino, S. H. Ahn, Z. Yang, S. G. Van Lanen, E. Boros, *J. Med. Chem.* **2019**, *62*, 9947–9960; c) A. Pandey, M. Cao, E. Boros, *ACS Infect. Dis.* **2022**, *8*, 878–888; d) M. Ghosh, P. A. Miller, M. J. Miller, *J. Antibiot.* **2020**, *73*, 152–157; e) C. Ji, M. J. Miller, *BioMetals* **2015**, *28*, 541–551.
[13] B. D. Bax, G. Murshudov, A. Maxwell, T. Germe, *J. Mol. Biol.* **2019**, *431*, 3427–3449.
[14] T. Zheng, J. L. Bullock, E. M. Nolan, *J. Am. Chem. Soc.* **2012**, *134*, 18388–18400.
[15] I. Schneider, Universität Konstanz **2016**.
[16] T. A. Wencewicz, T. E. Long, U. Mollmann, M. J. Miller, *Bioconjugate Chem.* **2013**, *24*, 473–486.
[17] K. N. Raymond, B. E. Allred, A. K. Sia, *Acc. Chem. Res.* **2015**, *48*, 2496–2505.
[18] a) I. G. Young, L. Langman, R. K. Luke, F. Gibson, *J. Bacteriol.* **1971**, *106*, 51–57; b) M. Sakaitani, F. Rusnak, N. R. Quinn, C. Tu, T. B. Frigo, G. A. Berchtold, C. T. Walsh, *Biochemistry* **1990**, *29*, 6789–6798.
[19] a) B. Troxell, H. M. Hassan, *Front. Cell. Infect. Microbiol.* **2013**, *3*, 59; b) M. A. McIntosh, C. F. Earhart, *J. Bacteriol.* **1977**, *131*, 331–339.
[20] R. Liu, P. A. Miller, S. B. Vakulenko, N. K. Stewart, W. C. Boggess, M. J. Miller, *J. Med. Chem.* **2018**, *61*, 3845–3854.
[21] a) C. Ji, P. A. Miller, M. J. Miller, *ACS Med. Chem. Lett.* **2015**, *6*, 707–710; b) C. Peukert, A. C. Vetter, H. L. S. Fuchs, K. Harmrolfs, B. Karge, M. Stadler, M. Brönstrup, *Chem. Sci.* **2023**, *14*, 5490–5502, doi: 10.1039/D2SC06850H.
[22] A. Brezden, M. F. Mohamed, M. Nepal, J. S. Harwood, J. Kuriakose, M. N. Seleem, J. Chmielewski, *J. Am. Chem. Soc.* **2016**, *138*, 10945–10949.
[23] T. A. Wencewicz, U. Mollmann, T. E. Long, M. J. Miller, *BioMetals* **2009**, *22*, 633–648.
[24] a) W. Tegge, G. Guerra, A. Höltke, L. Schiller, U. Beutling, K. Harmrolfs, L. Gröbe, H. Wullenkord, C. Xu, H. Weich, M. Brönstrup, *Angew. Chem. Int. Ed. Engl.* **2021**, *60*, 17989–17997; b) J. Meiers, K. Rox, A. Titz, *J. Med. Chem.* **2022**, *65*, 13988–14014.
[25] H. Prochnow, V. Fetz, S. K. Hotop, M. A. García-Rivera, A. Heumann, M. Brönstrup, *Anal. Chem.* **2019**, *91*, 1863–1872.
[26] M. Brönstrup, D. Schröder, I. Kretzschmar, C. A. Schalley, H. Schwarz, *Eur. J. Inorg. Chem.* **1998**, 1529–1538.
[27] a) M. Brönstrup, D. Schröder, H. Schwarz, *Chem. Eur. J.* **2000**, *6*, 91–104; b) M. Brönstrup, C. Trage, D. Schröder, H. Schwarz, *J. Am. Chem. Soc.* **2000**, *122*, 699–704; c) M. Brönstrup, D. Schröder, H. Schwarz, *Can. J. Chem.* **1999**, *77*, 774–780; d) M. Brönstrup, D. Schröder, H. Schwarz, *Chem. Eur. J.* **1999**, *5*, 1176–1185; e) M. Brönstrup, I. Kretzschmar, D. Schröder, H. Schwarz, *Helv. Chim. Acta* **1998**, *81*, 2348–2369.

Manuscript received: March 22, 2023
Revised manuscript received: June 28, 2023
Version of record online: July 19, 2023